12-4-2008

Fingering Instabilities on Reaction Fronts in the CO Oxidation Reaction on Pt(100)

D. Bilbao

Jochen A. Lauterbach
University of South Carolina - Columbia, lauteraj@cec.sc.edu

Publication Info

New Journal of Physics, Volume 10, 2008, pages 123002-.

Fingering instabilities on reaction fronts in the CO oxidation reaction on Pt(100)

New Journal of Physics
The open-access journal for physics

Fingering instabilities on reaction fronts in the CO oxidation reaction on Pt(100)

D Bilbao and J Lauterbach
Center for Catalytic Science and Technology, Department of Chemical Engineering, University of Delaware, Newark, DE 19716, USA
E-mail: lauterba@udel.edu

New Journal of Physics **10** (2008) 123002 (10pp)
Received 30 July 2008
Published 4 December 2008
Online at http://www.njp.org/
doi:10.1088/1367-2630/10/12/123002

Abstract. Fingering instabilities arising from local perturbations to planar reaction fronts in the CO oxidation reaction on Pt(100) are presented. CO oxidation represents a heterogeneous nonlinear system with the necessary kinetic and diffusive transport properties to support the development of fingered wave fronts. External forcing was utilized to create CO wave fronts on an otherwise monostable, O-covered surface, which, upon destabilization, gave rise to fingers of adsorbed CO extending into the O adlayer ahead of the reaction front. Finger spreading and tip-splitting were observed as the finger pattern evolved towards an intrinsic wavelength, independent of the length of the reaction front, calculated to be approximately 40 μm. Our data also show the presence of a shielding process, where at wavelengths less than twice the observed intrinsic value, additional fingers were created on the reaction front through a tip-splitting bifurcation of an existing finger. At wavelengths greater than twice the intrinsic value, additional fingers formed in the troughs between adjacent fingers, apparently unaffected by the presence of the larger surrounding fingers.

Contents

1. Introduction

Instabilities on planar interfaces separating two phases in nonlinear systems have the potential to grow into large perturbations characterized by cellular structures, or fingers, extending from the interface. Such finger patterns have been observed in numerous systems with distinct physical backgrounds. Many experimental and theoretical studies have focused on the onset and growth of finger structures in Hele–Shaw cells, where a less viscous fluid displaces a fluid of higher viscosity [1]–[3]. Depending on the physical properties of the fluids involved and the orientation of the experimental cell, a variety of patterned wave fronts can develop over a range of length scales due to finger shielding, spreading, and tip-splitting. Cellular fronts have also been documented in the directional solidification of alloys, where crystalline fingers grew into the liquid phase ahead of the eutectic interface according to scaling laws similar to those governing the growth of viscous fingers in the Hele–Shaw system [4]. Nonlinear reaction–diffusion systems may also produce interfacial patterns, provided the system involves the right combination of reaction kinetics and diffusive transport [5, 6]. The chemical reaction must involve an autocatalytic step where the formation of a particular species enhances its own rate of production. Also, the mobility of key species within the reaction medium must differ sufficiently. A reactant which diffuses faster than the autocatalytic species will act to destabilize a perturbed planar wave front, whereas rapid diffusion of the autocatalytic species tends to restore the planar geometry.

Here we investigate the destabilization of reaction fronts due to diffusive instabilities in the heterogeneous catalytic reaction of CO and O_2 on Pt(100). The CO oxidation reaction is well known to proceed via Langmuir–Hinshelwood type kinetics and satisfies the criteria listed above for the destabilization and growth of perturbations on a reaction interface [7]. The system exhibits bistability, and can exist in a highly-reactive, oxygen covered state, or a CO poisoned state where the catalytic activity is low due to blocking of O_2 adsorption sites by adsorbed CO [8]–[10]. The feedback mechanism, which allows the system to alternate between these two kinetic branches giving rise to rate oscillations and spatio-temporal patterns, is a periodic restructuring of the Pt surface atoms between a 1×1 and a quasi-hexagonal (hex) orientation [11, 12]. Autocatalysis is supplied through the dissociative adsorption of oxygen on the surface, where each O adatom goes on to react with an adsorbed CO molecule to form two CO_2 species. The CO_2 quickly desorbs from the surface leaving behind two open adsorption sites in exchange of the original single site. In the presence of excess gas-phase O_2, this doubling

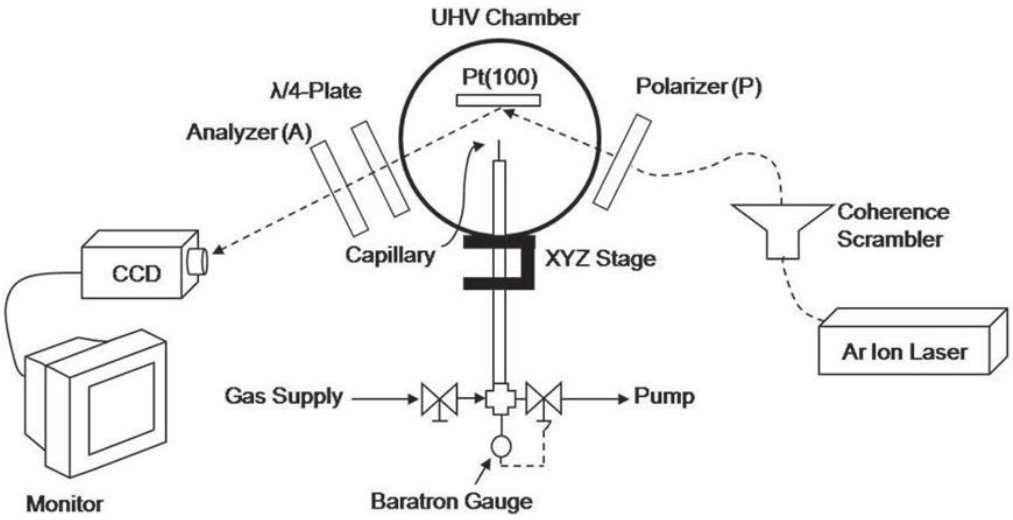

Figure 1. Diagram of experimental setup including EMSI components and local gas doser used to locally perturb the surface reaction.

of adsorption sites leads to autocatalytic oxygen waves which propagate across the surface [13]. Lastly, due to a higher binding energy on Pt, O is less mobile on the surface compared to adsorbed CO [14]. At the temperatures of interest in this study, the ratio of surface diffusion coefficients for CO and O is of the order of 10^{10} [15], which is sufficient to amplify small disturbances on the reaction front. The sections that follow discuss the development of these disturbances into fingers of adsorbed CO, which grow perpendicular to the reaction front into the O adlayer. The subsequent spreading and tip-splitting of the fingers is also reviewed as a potential pathway for attaining a characteristic wavelength determined by the reaction–diffusion properties of the CO oxidation system.

2. Experimental

Experiments were carried out on a Pt(100) single crystal mounted in a stainless steel ultra-high vacuum (UHV) chamber containing reactants at constant pressure. The sample was heated resistively by passing current through two Ta wires spotwelded to the back of the sample. A type-K thermocouple attached to the sample was used to monitor the sample temperature. The Pt surface was cleaned by repeated cycles of annealing to 1200 K, Ar ion sputtering under 1×10^{-4} Torr Ar, and oxidation at 950 K and 1×10^{-6} Torr O_2. The catalyst surface was continuously analyzed using ellispomicroscopy for surface imaging (EMSI), which detects different adsorbates based on local changes in the optical properties of the surface [16]. A schematic of the experimental setup is shown in figure 1. Light from a 5 W Ar ion laser was transmitted via fiber optic cable to a Glan–Thompson polarizer (P) which linearly polarized the laser light entering the UHV chamber. Following reflection from the surface, the elliptically polarized light was passed through a $\lambda/4$-plate and a second polarizer (A) before impinging on a CCD camera which recorded the data to a digital video recorder (DVR). The ellipsometer was configured such that CO-covered regions of the surface appear darker in relation to O-covered areas.

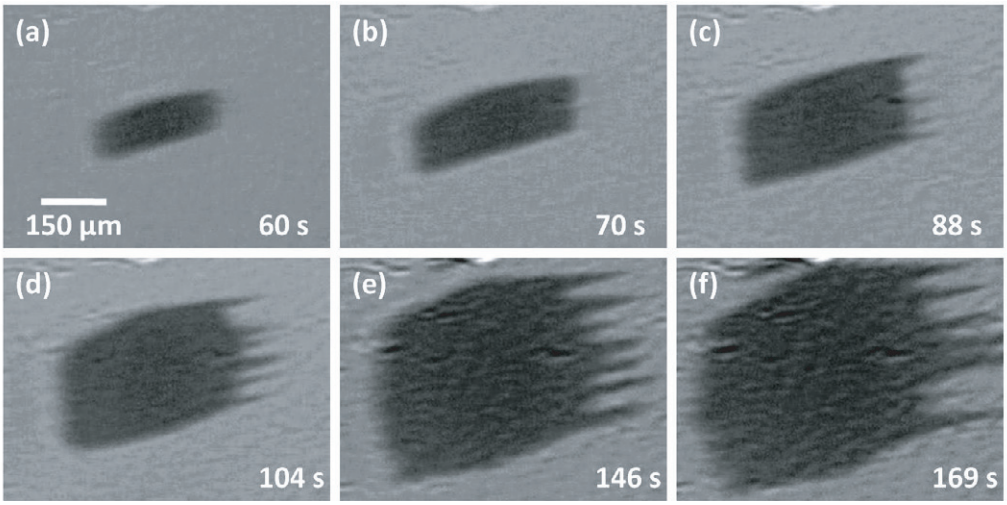

Figure 2. Fingering instability on a planar CO wave front. Figure 2(a) shows the initial CO island created by locally perturbing an O-covered surface under global reaction conditions of 403 K and 4×10^{-4} Torr O_2 with CO. Figures 2(b)–(e) illustrate the onset and development of fingers of adsorbed CO extending out into the unperturbed O adlayer.

External forcing was used to locally perturb the surface and create reaction fronts under global reaction conditions which do not typically support the formation of spontaneous chemical fronts. This was done by locally dosing gas onto the surface via a capillary tube positioned 500 μm from the surface. A glass capillary with a square shaped internal channel with a cross-sectional area of 2500 μm^2 was used to promote the development of a square shaped perturbation on the surface, thereby creating the necessary planar wave fronts which preceeded the fingering instability. The local gas doser was mounted on an x–y–z manipulator for precision movement and was supplied with reactant maintained at a desired pressure to control the intensity of the surface perturbation.

The catalyst surface was characterized using a JEOL 7400f scanning electron microscope (SEM). To ensure surface regions imaged with SEM were the same as those imaged using EMSI, regions of interest were first located in the UHV reactor by measuring the distance between the region and neighboring defects using the ellipsomicroscope to monitor the travel of the sample. The sample was then transferred from the UHV reactor to the SEM where particular defects were located with the SEM and the sample was positioned accordingly to reproduce the orientation of the sample in the UHV reactor.

3. Diffusive instabilities on CO wave fronts

Prior to local perturbation, a stable O-covered surface was prepared at a catalyst temperature of 403 K with a global O_2 pressure of 4×10^{-4} Torr. The local gas doser was positioned above the EMSI field of view, and CO flowed through the capillary towards the surface. The relatively high local concentration of CO in the gas phase reacted away adsorbed O in front of the capillary, resulting in an island of adsorbed CO surrounded by the unperturbed O adlayer as shown in figure 2(a). The square shape of the CO island reflects the geometry of the capillary channel used

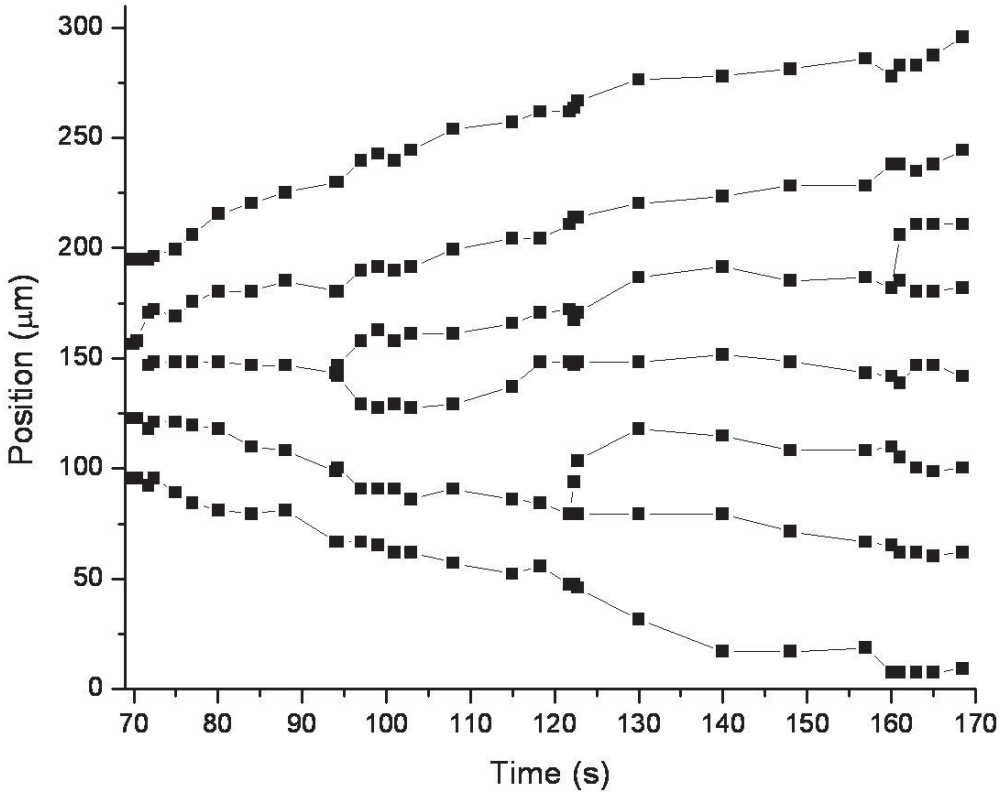

Figure 3. Space-time behavior of the CO fingers shown in figure 2. Each data point denotes the position of the tip of the respective CO finger as the finger pattern developed.

to control the molecular CO stream, and was maintained by the low surface temperature which minimized surface diffusion. As the CO island grew and expanded into the O adlayer, defects on the surface varied the local reaction–diffusion behavior of adsorbates, causing the planar front on the right side of the island to become unstable. The initial stages of the instability are depicted in figure 2(b), where four CO fingers, roughly 10 μm in amplitude with a wavelength of 30 μm, have developed on the reaction front. The ever increasing length of the reaction front, due to the expansion of the CO island, caused continuous rearrangement and spreading of the fingers along the interface. This behavior is illustrated in figures 3 and 4, which show the spatial position of the CO finger tips and the average wavelength (λ_{avg}) of the fingers in time. The second data set shown in figure 4, as denoted by the open circles, plots the average wavelength scaled by the square of the reaction front length (L) measured from the tips of the two outermost fingers. Shortly after the appearance of the fingering instability in figure 2(b), the second finger from the top of the reaction front underwent a tip-splitting bifurcation, giving rise to a fifth finger on the wave front decreasing λ_{avg} to 25 μm. After an initial rearrangement period, the five CO fingers were distributed along the reaction front as shown in figure 2(c), where the amplitude of the fingers had grown to 60 μm and λ_{avg} was now 36 μm. At this point, the rate of finger spreading decreased and remained constant for the following 10 s. Near 90 s, the spreading rate again increased just before the center finger split, leaving six fingers on the reaction front (figure 2(d)). Similar trends in the spreading and tip-splitting dynamics of the CO fingers can

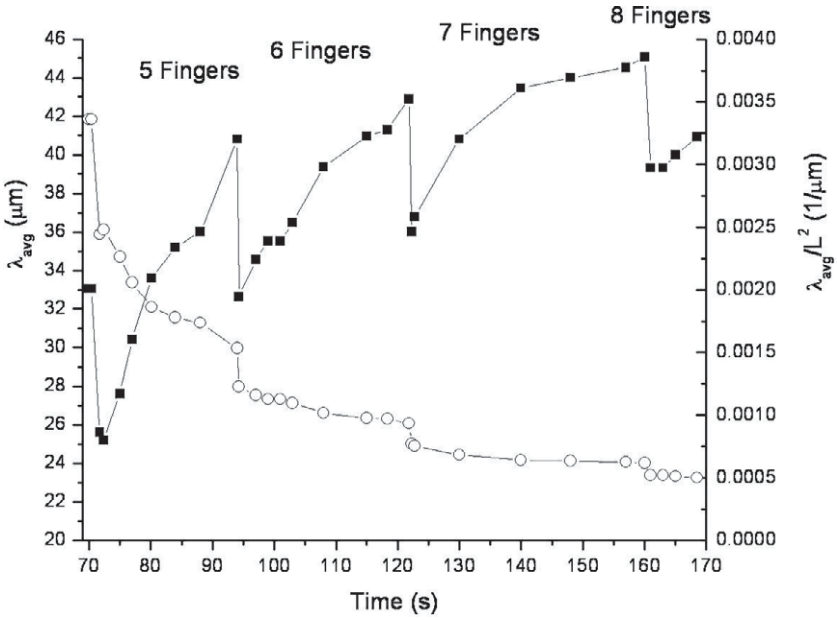

Figure 4. Evolution of the average finger wavelength (λ_{avg}) (square data points) and the scaled average wavelength of the finger pattern shown in figure 2. The scaled wavelength is calculated as λ_{avg} divided by the square of the reaction front length (L), where L is measured as the distance between the two outermost CO finger-tips.

be seen in figure 2(b) for the subsequent formation of a seventh (figure 2(e)) and eighth finger (figure 2(f)) on the reaction front.

The observed spreading and periodic splitting of the CO fingers as the reaction front lengthened suggests that these two processes are interdependent. The formation of additional fingers on the reaction front following a tip-splitting bifurcation temporarily contributed to the lengthening of the front due to finger spreading. Likewise, the continuously increasing length of the reaction front as the CO island expanded also acted to spread the fingers along the reaction front. Eventually, two fingers on either side of a given finger (e.g. fingers 2 and 4 in the five finger region) surpassed a critical spacing from the center finger, at which point the middle finger split and the spreading process was repeated. In figure 4, λ looks to be somewhat influenced by L initially, but, due to the unique presence of a continuously growing reaction front, begins to approach a constant, intrinsic value independent of L. Based on the decay of the scaled wavelength in figure 4, this intrinsic wavelength is calculated to be on the order of 40 μm and represents the spacing the fingers would exhibit in the case of an infinite reaction front length. Such intrinsic length scales are common to diffusive systems which exhibit spatially modulated patterning, such as those arising from a Turing type bifurcation [17, 18], and are completely determined by the reaction–diffusion properties of the system [6, 19].

4. Destabilization of the reaction front

Local perturbations are crucial in the initial destabilization of the planar interface. The intensity as well as the length scale of the perturbation determines whether the local disturbance will

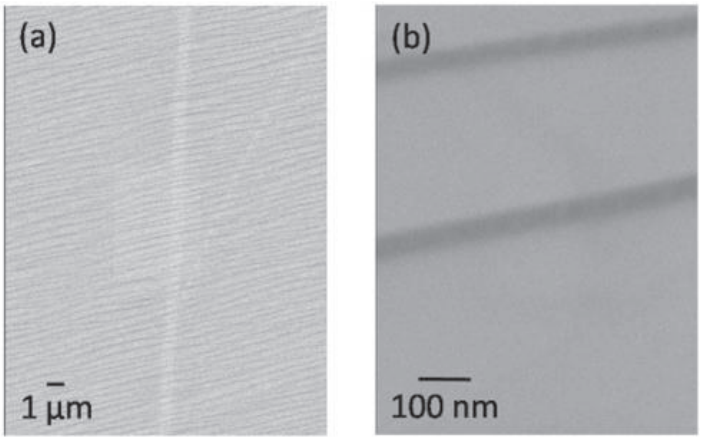

Figure 5. SEM images of the Pt surface where fingering instabilities were observed. Figure 5(a) shows the surface to consist of many long parallel plateaus, corresponding to the lighter regions of the image, separated by narrow valleys. Figure 5(b) provides a higher magnification image of the plateau surface morphology.

develop or decay without impacting the dynamics of the system [19]–[21]. Local perturbations can be present in the form of random heterogeneities in the experimental apparatus [22], which locally alter the dynamic behavior of key species, or, in the case of theoretical studies, applied through the addition of random noise or a particular wave form on the interface [6, 23]. In heterogeneous catalytic systems, local perturbations to the system are often the result of heterogeneities or defects in the arrangement of surface atoms. Such variations in the structure of the catalytic surface will modify the way in which reactants adsorb, diffuse and react on the surface, thereby influencing the overall dynamic behavior of the system [24, 25].

To better understand the role of the catalyst surface in the development of the fingering instability, the single crystal surface was analyzed using scanning electron microscopy. The SEM images, included in figure 5, demonstrate that the surface consists of plateau features (lighter contrasting regions), approximately 250 nm wide, separated by parallel running valleys (darker contrasting regions) approximately 50 nm in width. The alignment of the plateaus on the surface is parallel to the growth direction of the fingers shown in figure 2, however, the length scale of this surface morphology is clearly beneath that of the observed finger structures. For instance, the second CO finger from the top of the seven fingered front in figure 2(e) had a full-width half-maximum (FWHM) value of 30 μm and a baseline width of the order of 50 μm. Therefore, this finger perturbation spans around 200 plateau structures at its baseline. From this comparison, it can be concluded that the contribution of this surface morphology to the formation of patterned fronts is limited to the initial perturbation of the planar reaction front. Precisely how the reaction front is destabilized by the plateau morphology is not clear at this time. Although, based on the affinity of O_2 towards surface defects and step edges [26], it is possible that an enhanced O presence at the edges of each plateau offsets the rapid diffusion of CO across the interior region of the plateau. These two opposing processes could lead to a modulation of the reaction front, which in turn, due to the nature of the surface reaction, could result in the growth of finger structures parallel to the surface plateaus.

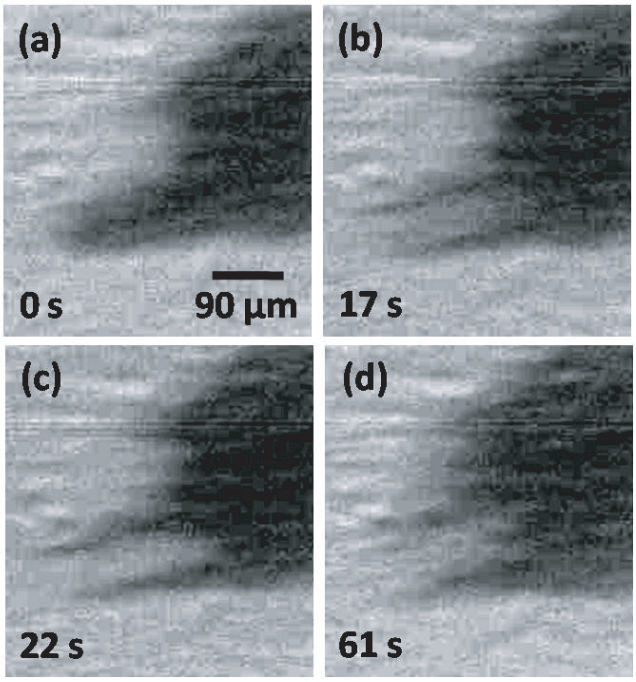

Figure 6. Images detailing the tip-splitting of a CO finger (6(a)–(c)) and the subsequent formation of an additional finger in the trough between two fingers (6d)). Global reaction conditions: $T = 433$ K, $p_{O_2} = 5 \times 10^{-4}$ Torr.

5. Analysis of finger-tip splitting

Although the fingers presented in figure 2 are easily resolved with EMSI, many of the tip-splitting events in this experiment take place at the lower spatial resolution limit of the ellipsomicroscope, making it difficult to study the bifurcation in detail. As such, we present an analysis of the tip-splitting of larger fingers, such as that shown in figure 6(a), which presumably are representative of bifurcations occurring on smaller scales. The finger shown in figure 6(a) developed on a reaction boundary which was initiated by locally perturbing an O-covered surface at 433 K under 5×10^{-4} Torr O_2 with CO. This particular finger grew to a maximum amplitude of 100 μm with a FWHM of 80 μm. The initial splitting of the finger began with the formation of an oxygen wave just to the right of the finger centerline. The O wave then traveled into the surface region occupied by the CO finger, reacting away adsorbed CO and leaving the surface in an O-covered state (figure 6(b)). Remarkably, the oxygen wave only removed CO from the interior region of the CO finger, leaving behind two CO fingers on either side of the now O-covered surface region. The amplitude of the two newly formed CO fingers is similar to that of the original single finger, however, the fingers are significantly sharper having FWHM values of the order of 25 μm, which is near the FWHM values of the fingers presented in figure 2. The O wave continued to propagate and divide the CO finger until the supply of CO to the reaction front halted the advancing O wave. As shown in figure 6(c), this stopping point is consistent with the location of the CO/O interface elsewhere on the CO island. The two CO fingers shown in figure 6(c) were separated by a distance of 70 μm, and slowly migrated to a distance of 80 μm over the next 40 s (figure 6(d)). Once the wavelength reached 80 μm, a third

finger was observed growing in at the trough between the two CO fingers. The growth of this additional finger is significant as, aside from the initial front destabilization, additional fingers were normally created on the reaction front as a result of the tip-splitting of existing fingers. Here, the selective growth of an additional finger in the trough position again implicates the existence of an intrinsic pattern wavelength near 40 μm. For systems where $\lambda < \lambda_c$, as is the case for the front shown in figure 2, tip-splitting is the dominant mechanism for the formation of additional fingers as existing fingers on an already crowed reaction front shield the growth of new smaller fingers attempting to form in the trough between adjacent fingers. Alternatively, when $\lambda \geqslant 2^*\lambda_c$, a relation previously found to be significant in the dynamics of fingered fronts elsewhere [3, 27], shielding is no longer a factor and smaller fingers are able to develop in between larger adjacent fingers as illustrated in figure 6(d).

6. Conclusions

Fingering instabilities on planar CO fronts in the oxidation of CO on Pt(100) were examined. To the best of our knowledge, this is the first observation of such behavior in a heterogeneous reaction–diffusion system. The onset and development of the fingering instability is attributed to the particular reaction–diffusion properties of the surface reaction paired with the use of external forcing to create reaction fronts under otherwise monostable global reaction conditions. Local reaction rate perturbations to CO wave fronts, provided by a catalyst surface morphology made up of parallel plateau structures, destabilized the propagating reaction fronts leading to fingers of adsorbed CO which extended into the O adlayer ahead of the wave front. Finger spreading and tip-splitting were observed as a means of attaining an intrinsic finger wavelength, calculated to be on the order of 40 μm for relatively large reaction fronts. Additional analysis of the finger tip-splitting bifurcation suggests shielding is dominant when the spacing between fingers is less than the intrinsic value, with smaller fingers collapsing into larger finger structures on the front. For finger wavelengths twice the intrinsic value, additional fingers were observed developing in the trough between existing fingers, apparently unaffected by their presence. Currently, computational studies which combine physically realistic reaction–diffusion parameters with the observed surface morphology are underway to provide additional insight into the dynamics of the observed fingering instability.

Acknowledgments

We acknowledge the donors of the American Chemical Society Petroleum Research Fund and the US Department of Energy for support (or partial support) of this research, and Dr C M Snively for many fruitful discussions.

References

[1] Saffman P G and Taylor G 1958 *Proc. R. Soc.* A **245** 312
[2] Homsy G M 1987 *Annu. Rev. Fluid Mech.* **19** 271
[3] Tan C T and Homsy G M 1988 *Phys. Fluids* **31** 1330
[4] Trivedi R, Liu S and Williams S 2002 *Nat. Mater.* **1** 157
[5] Horvath D and Toth A 1988 *J. Chem. Phys.* **108** 1447
[6] Horvath D, Petrov V, Scott S K and Showalter K 1993 *J. Chem. Phys.* **98** 6332

[7] Engel T and Ertl G 1979 *Adv. Catal.* **28** 1
[8] Slin'ko M M and Jaegar N I 1994 *Oscillating Heterogeneous Catalytic Systems* (Amsterdam: Elsevier)
[9] Imbihl R, Cox M P, Ertl G, Muller H and Brenig W 1985 *J. Chem. Phys.* **83** 1578
[10] Imbihl R, Cox M P and Ertl G 1986 *J. Chem. Phys.* **84** 3519
[11] Heinz K, Lang E, Strauss K and Muller K 1982 *Appl. Surf. Sci.* **11–12** 611
[12] Norton P R, Da Vies J A, Creber D K, Sitter C W and Jackman T E 1981 *Surf. Sci.* **108** 205
[13] Lauterbach J and Rotermund H H 1994 *Surf. Sci.* **311** 231
[14] Barteau M A, Ko E I and Madix R J 1981 *Surf. Sci.* **102** 99
[15] von Oertzen A, Mikhailov A, Rotermund H H and Ertl G 1996 *Surf. Sci.* **350** 259
[16] Rotermund H H, Haas G, Franz R U, Tromp R M and Ertl G 1995 *Science* **270** 608
[17] Yang L, Dolnik M, Zhabotinsky A M and Epstein I R 2006 *Chaos* **16** 037114
[18] Castets V, Dulos E, Boissonade J and De Kepper P 1990 *Phys. Rev. Lett.* **64** 2953
[19] Epstein I R and Pojman J A 1998 *An Introduction to Nonlinear Chemical Dynamics* (New York: Oxford University Press)
[20] Horvath D and Toth A 1997 *J. Chem. Soc. Faraday Trans.* **93** 4301
[21] Horvath D, Monika K and Toth A 1998 *J. Chem. Soc. Faraday Trans.* **94** 1217
[22] Tabeling P, Zocchi G and Libchaber A 1987 *J. Fluid Mech.* **177** 67
[23] Zimmerman W B and Homsy G M 1991 *Phys. Fluids* A **3** 1859
[24] Falta J, Imbihl R, Sander M and Henzler M 1992 *Phys. Rev.* B **45** 6858
[25] Gottschalk N, Mertens F, Bar M, Eiswirth M and Imbihl R 1994 *Phys. Rev. Lett.* **73** 3483
[26] Ladas S, Imbihl R and Ertl G 1998 *Surf. Sci.* **197** 153
[27] Lima D, D'Onofrio A and De Wit A 2006 *J. Chem. Phys.* **124** 014509